

This is a self-archived version of an original article. This version may differ from the original in pagination and typographic details.

Author(s): Koehler, Birgit; Powers, Leanne C.; Cory, Rose M.; Einarsdóttir, Karólína; Gu, Yufei; Tranvik, Lars J.; Vähätalo, Anssi V.; Ward, Collin P.; Miller, William L.

Title: Inter-laboratory differences in the apparent quantum yield for the photochemical production of dissolved inorganic carbon in inland waters and implications for photochemical rate modeling

Year: 2022

Version: Published version

Copyright: © 2022 the Authors










Rights: CC BY-NC-ND 4.0

Rights url: <https://creativecommons.org/licenses/by-nc-nd/4.0/>

Please cite the original version:

Koehler, B., Powers, L. C., Cory, R. M., Einarsdóttir, K., Gu, Y., Tranvik, L. J., Vähätalo, A. V., Ward, C. P., & Miller, W. L. (2022). Inter-laboratory differences in the apparent quantum yield for the photochemical production of dissolved inorganic carbon in inland waters and implications for photochemical rate modeling. *Limnology and Oceanography : Methods*, 20(6), 320-337.
<https://doi.org/10.1002/lom3.10489>

Inter-laboratory differences in the apparent quantum yield for the photochemical production of dissolved inorganic carbon in inland waters and implications for photochemical rate modeling

Birgit Koehler ^{1,a,*} Leanne C. Powers ^{2,b} Rose M. Cory ³ Karólína Einarsdóttir ¹ Yufei Gu ⁴
Lars J. Tranvik ¹ Anssi V. Vähätalo ⁴ Collin P. Ward ^{3,c} William L. Miller ^{2,*}

¹Ecology and Genetics/Limnology, Evolutionary Biology Centre, Uppsala University, Uppsala, Sweden

²Department of Marine Sciences, University of Georgia, Athens, Georgia

³Earth and Environmental Sciences, University of Michigan, Ann Arbor, Michigan

⁴Department of Biological and Environmental Science, University of Jyväskylä, Jyväskylä, Finland

Abstract

Solar radiation initiates photochemical oxidation of dissolved organic carbon (DOC) to dissolved inorganic carbon (DIC) in inland waters, contributing to their carbon dioxide emissions to the atmosphere. Models can determine photochemical DIC production over large spatiotemporal scales and assess its role in aquatic C cycling. The apparent quantum yield (AQY) spectrum for photochemical DIC production, defined as mol DIC produced per mol chromophoric dissolved organic matter-absorbed photons, is a critical model parameter. In previous studies, the principle for the determination of AQY spectra is the same but methodological specifics differ, and the extent to which these differences influence AQY spectra and simulated aquatic DIC photo-production is unclear. Here, four laboratories determined AQY spectra from water samples of eight inland waters that are situated in Alaska, Finland, and Sweden and span a nearly 10-fold range in DOM absorption coefficients. All AQY values fell within the range previously reported for inland waters. The inter-laboratory coefficient of variation (CV) for wavelength-integrated AQY spectra (300–450 nm) averaged $38\% \pm 3\%$ SE, and the inter-water CV averaged $63\% \pm 1\%$. The inter-laboratory CV for simulated photochemical DIC production (conducted for the five Swedish lakes) averaged $49\% \pm 12\%$, and the inter-water CV averaged $77\% \pm 10\%$. This uncertainty is not surprising given the complexities and methodological choices involved in determining DIC AQY spectra and needs to be considered when applying photochemical rate modeling. Thus, we also highlight current methodological limitations and suggest future improvements for DIC AQY determination to reduce inter-laboratory uncertainty.

*Correspondence: birgit.koehler@slu.se, bmiller@uga.edu

Author Contribution Statement: BK designed this study, in discussion with all coauthors. KE, AV and RC sampled water in Sweden, Finland and Alaska, respectively. KE prepared water samples of each study lake for distribution to the four involved laboratories. KE, YG, CW, LP and BM conducted the measurements of AQY spectra, with assistance of the other authors. All authors were involved in calculating AQY spectra from their respective laboratories. BK compiled the data from all laboratories, conducted statistical analyses, and prepared figures and tables. BK and LP wrote the manuscript. All authors discussed throughout the study and during manuscript preparation, and commented on manuscript drafts.

^aBirgit Koehler and Leanne C. Powers contributed equally to this study.

Associate editor: Hayley Schiebel

Additional Supporting Information may be found in the online version of this article.

This is an open access article under the terms of the Creative Commons Attribution-NonCommercial-NoDerivs License, which permits use and distribution in any medium, provided the original work is properly cited, the use is non-commercial and no modifications or adaptations are made.

^aPresent address: Department of Aquatic Resources, Institute of Coastal Research, Swedish University of Agricultural Sciences, Uppsala, Sweden

^bPresent address: Department of Chemistry, State University of New York College of Environmental Science and Forestry, Syracuse, New York

^cPresent address: Department of Marine Chemistry and Geochemistry, Woods Hole Oceanographic Institution, Woods Hole, Massachusetts

Globally, lakes and reservoirs emit 0.3–0.6 Gt C yr⁻¹ as carbon dioxide (CO₂) to the atmosphere (Cole et al. 2007; Raymond et al. 2013; Drake et al. 2018). Some CO₂ emitted from inland waters results from photochemical mineralization of dissolved organic carbon (DOC) to dissolved inorganic carbon (DIC) (Granéli et al. 1996; Gao and Zepp 1998; Cory et al. 2014). Photochemical mineralization of DOC globally generates annual C fluxes similar in magnitude to C burial in natural lake sediments (Koehler et al. 2014) and may account for 3% to up to ca. 30% of CO₂ emitted from arctic and boreal lakes (Cory et al. 2014; Groeneveld et al. 2016; Vachon et al. 2016; Allesson et al. 2021).

Photochemical production of CO₂ from inland waters is often estimated from spectral photochemical rate modeling (Fichot and Miller 2010; Aarnos et al. 2012; Cory et al. 2014; Koehler et al. 2014). A key parameter in the model is the photochemical reactivity of dissolved organic matter (DOM), quantified as the apparent quantum yield (AQY). The AQY is defined as mol DIC photochemically produced per mol photons absorbed by chromophoric DOM (CDOM).

The methodologies for the determination of AQYs vary substantially in the literature. One method uses monochromatic radiation at specific wavelengths to determine AQY spectra for DIC production from CDOM (Gao and Zepp 1998; Vähätalo et al. 2000; Bowen et al. 2020). A limitation to the monochromatic method is that the total photochemical DIC production can be very small due to the limited photon flux within a small bandwidth. Although recent advances in light-emitting diode technology, creating narrow-band photon emission, have overcome this limitation (Bowen et al. 2020; Ward et al. 2021), prior research using monochromatic AQY methods were only feasible in high CDOM waters or at high energy (ultraviolet-B radiation, UV-B) wavelengths where DIC yields from CDOM are highest.

Many recent studies determining spectral DIC AQYs are using DOM-exposure to polychromatic (i.e., broadband) light sources, often in combination with multiple optical cut-off filters (Johannessen and Miller 2001; Koehler et al. 2014), or by using natural sunlight (Vähätalo et al. 2000; Cory et al. 2013). The advantages and disadvantages of monochromatic vs. polychromatic AQY determination have recently been reviewed in detail elsewhere (Ward et al. 2021). One primary advantage of the polychromatic light is that it is representative of how CDOM is exposed to sunlight in natural waters, and thus may capture interactions between wavelengths (Cullen and Neale 1994) that produce DIC from CDOM. In addition, polychromatic light exposures for AQY can be less time consuming than those using monochromatic light. A potentially critical limitation of the polychromatic approach is the requirement for an a priori assumption of the spectral shape of the AQY spectrum, since the data are fit using a predetermined equation, usually an exponential function. Using an assumed shape of the AQY spectrum is supported by the literature because both monochromatic and polychromatic methods suggest that the AQY of photochemical DIC production in sunlit waters is highest for the high-energy photons absorbed in the

UV-B, and decreases toward longer wavelengths in the ultraviolet-A (UV-A) and visible ranges (Gao and Zepp 1998; Vähätalo et al. 2000; Johannessen and Miller 2001). However, it should be noted that some studies have found that other functions (e.g., a quasi-exponential equation; Belanger et al. 2006; Xie et al. 2012) better described DIC AQYs in some cases.

Although the general methods for determining AQY spectra from polychromatic irradiation experiments are similar (boxes in Fig. 1), laboratory-specific setups and method specifics can differ substantially (text next to boxes in Fig. 1). This includes, for example, sample storage and preirradiation treatment, arrangement of the irradiated vessels in the solar simulator, number and transmission spectra of optical cut-off filters, radiation dose (i.e., irradiation intensity and time) and quantification of total DOM-absorbed photons, as well as the mathematical function and fitting procedure used to describe the spectral dependency of AQY (Cory et al. 2014; Powers and Miller 2015a; Groeneveld et al. 2016; Gu et al. 2017). Moreover, our knowledge of spatial and temporal variability for AQY spectra that leads to photochemical DIC production in inland waters remains poor (Vähätalo et al. 2000; Vähätalo and Wetzel 2004; Cory et al. 2014; Koehler et al. 2014; Groeneveld et al. 2016; Koehler et al. 2016). Hence, AQY spectra present a potentially considerable source of uncertainty in any estimates of photochemical CO₂ emissions, such as from large-scale modeling of photochemical DIC production. It is unclear to what extent the relatively large differences in published estimates of the role of photochemistry in aquatic DOC mineralization are due to real differences in these water samples or due to inter-laboratory variations in the method specifics used to determine DIC AQY spectra.

Given that (1) simulated photochemical DIC production is sensitive to both the magnitude and slope of the AQY spectrum (Fichot and Miller 2010; Cory et al. 2014; Koehler et al. 2014) and (2) large-scale model simulations are used to assess the importance of sunlight for carbon cycling in inland waters (Koehler et al. 2014; Allesson et al. 2021), there is a need for inter-calibration studies of AQY spectra across the methods used in different laboratories. Here, we compare the results from four separate laboratories (corresponding to the four affiliations of the authors of this study), each using published protocols for determining photochemical AQY spectra for the production of DIC in sunlit waters. Using a set of samples from eight diverse inland waters, we examine the variability in AQY spectra between waters and between laboratories, discuss implications for the modeling of aquatic carbon cycling, and make recommendations for future work.

Materials and procedures

Sampled inland waters

During 15–20 September 2014, 10 L surface water were sampled from seven lakes in Alaska, Finland, and Sweden, and from one creek in Alaska (Table 1) using high-density polyethylene (HDPE) carboys that were precleaned using established

procedures (Mannino et al. 2019). The samples from Alaska were filtered on the sampling day over 0.7- μm glass microfiber filters (Whatman GF/F, GE Healthcare, Buckinghamshire, UK). The samples from Finland and Sweden were kept dark and cold until filtration within 2 weeks over 1.2- μm glass microfiber (Whatman GF/C) and 0.2- μm membrane filters (Supor[®]-200, Pall Corporation, Ann Arbor, Michigan, USA). To minimize differences in the water subsamples that were subsequently shipped to the four laboratories, the water was filtered into one 10-L container first, and then mixed thoroughly before distributing into 2-L precleaned HDPE bottles. These samples were immediately shipped to the four laboratories dark and cold, and stored dark and cold (4°C) until further analysis within 1–5 months. Just before the irradiation experiments, the water samples were refiltered in each laboratory using precombusted glass fiber filters (Whatman GF/F, about 0.7 μm), or 0.2- μm membrane filters of different models, specifically track-etched polycarbonate filters (Nuclepore, Merck Millipore, Darmstadt, Germany; or Cyclopore, Whatman, GE Healthcare Life Sciences, UK), and polyethersulfone Supor[®]-200 filters (Pall Corporation, Ann Arbor, Michigan, USA).

Apparent quantum yield

All AQY spectra presented in this comparison were determined by measuring DIC produced with solar simulator irradiation in the laboratory, quantifying DOM-absorbed photons, and fitting an exponential function to these data to define a wavelength-resolved AQY spectrum. The laboratory-specific protocols for the four groups involved in this study have been described in detail previously (Cory et al. 2014; Powers and Miller 2015a; Groeneveld et al. 2016; Gu et al. 2017). In the laboratory at the University of Michigan, photochemical DIC production was not detectable for Toolik Lake underneath the high cut-off filters (>370 nm) relative to dark controls, and was therefore measured as photochemical oxygen consumption (relative to dark controls), assuming a 1 : 1 relationship between consumed O₂ and produced CO₂ (Cory et al. 2014; Ward and Corry 2020). Also, in the laboratory at the University of Michigan, flocculant material was noted in the water samples of some lakes following storage. Although all laboratories followed a similar general workflow, laboratory-specific protocols varied in the detail of specific setups and procedures (Fig. 1). Differences

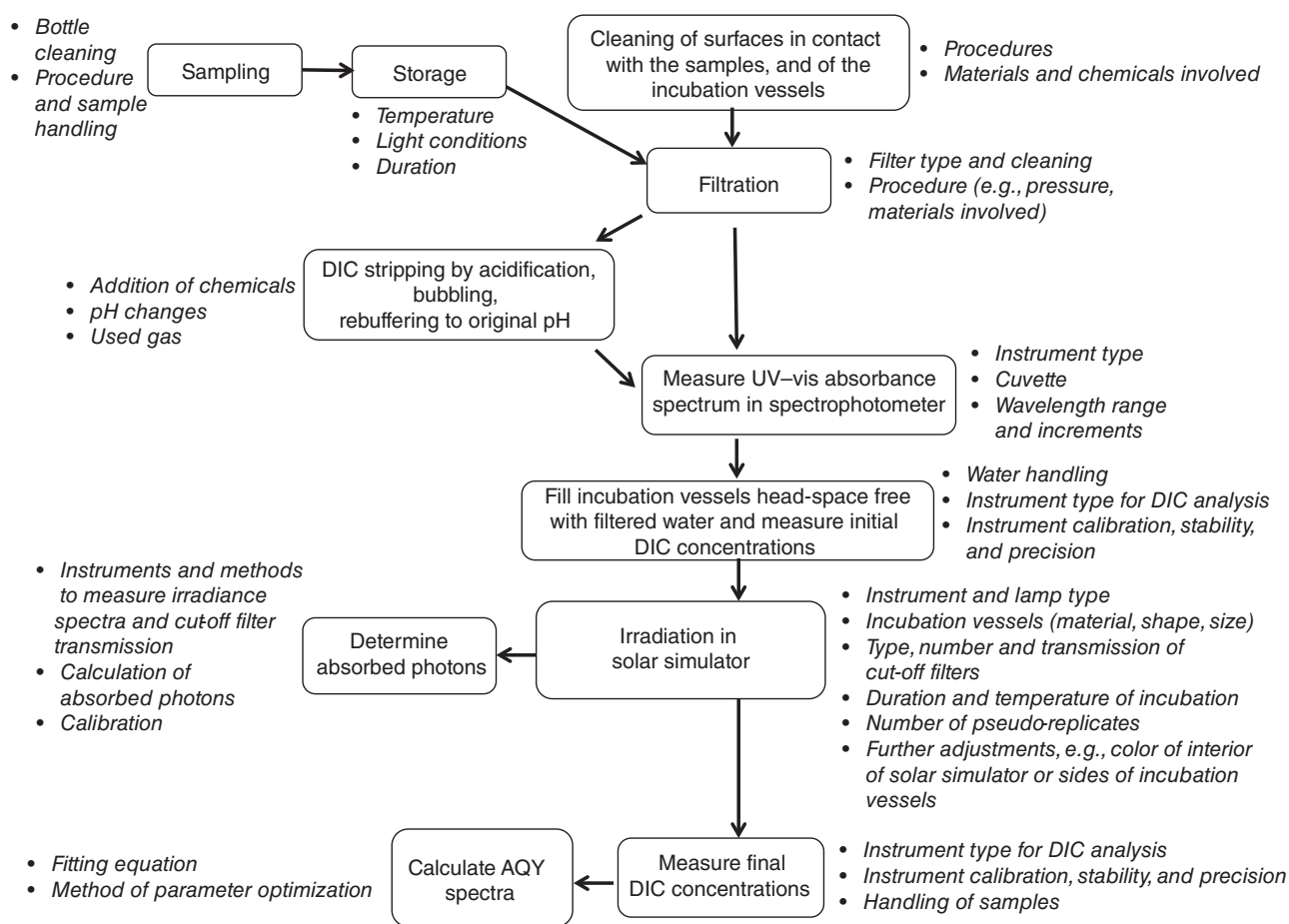


Fig. 1. Flow chart of steps involved in determining an AQY spectrum in the laboratory. Adjacent to the boxes naming the work steps are some of the aspects that may cause inter-laboratory differences. See Supporting Information Table S1 for details on how the central work steps were conducted in the four laboratories in this study. Work steps that were unified between laboratories in this study are described in the “Apparent quantum yield” section.

Table 1. Location and chemical water characteristics of the eight study lakes (mean \pm SE), sorted by ascending DOC concentrations*. For variables measured in all laboratories, that is, pH, $a_g(420)$, S_R , and CDOM, the inter-laboratory CV is also listed in parentheses. For pH values and optical properties measured in individual labs, see Supporting Information Table S4.

Lake	Location	WRT (months)	Mean depth (m)	DOC (mg L ⁻¹) (n = 1)	CDOM ₂₈₀₋₆₀₀ ($\times 10^{-7}$, unitless)			$a_g(420)$ (m ⁻¹) (n = 4)	S_R (n = 4)	pH (n = 4)	TDN (mg N L ⁻¹) (n = 1)	TDP (μ g P L ⁻¹) (n = 1)	TDFe (μ mol L ⁻¹) (n = 1)
					(n = 4)	(n = 4)	(n = 4)						
Toolik Lake, Alaska	68°37'N, 149°36'E	12	5.0	4.03	14.39 \pm 0.88 (12%)	2.15 \pm 0.22 (20%)	0.97 \pm 0.07 (14%)	7.5 \pm 0.3 (8%)	0.07	4	0.11		
Norra Bredsjön, Sweden	59°58'N, 15°10'E	19	7.3	7.80	30.25 \pm 1.45 (10%)	4.65 \pm 0.29 (12%)	0.91 \pm 0.01 (2%)	6.8 \pm 0.4 (12%)	0.11	7	1.18		
Övre Skärsjön, Sweden	59°50'N, 15°33'E	42	6.0	8.00	40.65 \pm 1.18 (6%)	6.55 \pm 0.25 (8%)	0.80 \pm 0.02 (5%)	6.1 \pm 0.1 (3%)	0.44	3	5.14		
Jyväsjärvi, Finland	62.14°N, 25.46°E	2.7	5.8	8.25	30.52 \pm 1.44 (9%)	4.47 \pm 0.26 (12%)	0.92 \pm 0.01 (2%)	7.0 \pm 0.3 (9%)	0.30	8	2.12		
Imnavait Creek, Alaska	68°37'N, 149°37'E	n.d.	0.5	9.72	44.54 \pm 1.33 (6%)	6.81 \pm 0.31 (9%)	0.78 \pm 0.04 (10%)	6.0 \pm 0.4 (13%)	0.32	8	6.69		
Gäddtjärn, Sweden	59°86'N, 15°18'E	2	3.4	11.00	61.20 \pm 1.87 (6%)	10.67 \pm 0.36 (7%)	0.86 \pm 0.01 (2%)	7.0 \pm 0.4 (11%)	0.35	17	5.51		
Grästjärn, Sweden	59°52'N, 15°07'E	1	<1	13.24	75.03 \pm 1.61 (4%)	12.40 \pm 0.55 (9%)	0.75 \pm 0.02 (5%)	5.8 \pm 0.2 (7%)	0.53	5	8.47		
Svartjärn, Sweden	59°89'N, 15°26'E	0.5	<1	21.55	135.82 \pm 1.87 (3%)	23.71 \pm 0.31 (3%)	0.78 \pm 0.02 (5%)	5.8 \pm 0.3 (10%)	0.73	4	15.06		

WRT, water retention time; S_R , slope ratio; n.d., not determined; TDN, total dissolved nitrogen; TDP, total dissolved phosphorus; TDFe, total dissolved iron.
* $a_g(420)$ is the absorption coefficient at 420 nm; CDOM as indicated by absorption coefficients integrated for 280–600 nm.

include (1) sample storage conditions and storage time, filtration and pretreatment; (2) type, size, shape, and orientation of the irradiation vessels; (3) optical measurements and assumptions; (4) irradiation time and photon flux; (5) the use or omission of optical cut-off filters to provide multiple DIC production rates that constrain AQY spectra; (6) the analysis of DIC concentrations preirradiation and postirradiation; and (7) mathematical fitting routines (Fig. 1; Supporting Information Table S1).

Apart from the laboratory at the University of Michigan, where no sample pretreatment was conducted, background DIC concentrations were reduced before irradiation. The water samples were acidified to $\text{pH} < 3$ using concentrated hydrochloric acid, bubbled using CO_2 -free air or nitrogen gas for 30–60 min, and sodium borate or sodium hydroxide was then added to readjust each sample to its original pH for irradiation. At Uppsala University, where nitrogen gas was used for bubbling, the water was reaerated during refiltration before irradiation, which resulted in significant oxygenation but only slightly increased the preirradiation DIC levels. At the University of Georgia laboratory, Imnavait Creek was not acidified before bubbling due to its original low pH and consequently low DIC baseline. Irradiation was conducted in solar simulators with 1.5, 1.7, or 1.8 kW Xenon lamps, specifically Suntest models CPS, CPS+, and XLS+ (Atlas Material Testing Technology, Mount Prospect, Illinois, USA), and a Q-Sun 1000 test chamber (Q-panel Lab Products Europe, Bolton, UK). DIC concentrations were determined directly from the incubation vessels using total organic carbon analyzers, specifically models TOC- V_{CPH} or TOC- L_{CPH} (Shimadzu Corporation, Kyoto, Japan) or Sievers 900 (General Electric Analytical Instruments, Manchester, UK), and a DIC analyzer model AS-C3 (Apollo SciTech, Newark, Delaware, USA). In the laboratory at the University of Georgia, the headspace created while removing sample for DIC analysis was replaced with CO_2 -free air passed through soda lime to prevent adding DIC from lab air.

DOM-absorbed photons ($Q_a(\lambda)$) were calculated as detailed in Supporting Information Table S1. While there were some differences in $Q_a(\lambda)$ calculations between laboratories, generally $Q_a(\lambda)$ was derived using measurements of spectral irradiance entering each sample and sample CDOM absorption coefficients. Generally, $Q_a(\lambda)$ is then calculated by solving a variation of the equation below

$$\frac{dQ_a(\lambda)}{dz} = E_0(\lambda) \times e^{(-a_t(\lambda) \times z)} \times a_g(\lambda) \times S, \quad (1)$$

where $E_0(\lambda)$ is collimated irradiance ($\text{mol photons m}^{-2} \text{ s}^{-1} \text{ nm}^{-1}$) at a given wavelength, λ , z is depth (m), $a_t(\lambda)$ is the total absorption coefficient (m^{-1}), $a_g(\lambda)$ is the CDOM absorption coefficient (m^{-1}), and S is the illuminated surface area (m^2) (Hu et al. 2002). In these filtered water samples $a_t(\lambda)$ should equal the sum of $a_g(\lambda)$ and $a_w(\lambda)$, where $a_w(\lambda)$ is the absorption coefficient of water.

Finally, across the four laboratories, the same exponential function was formulated in two different ways (Gu et al. 2017) to describe the AQY spectrum, specifically:

$$\text{AQY}(\lambda) = \frac{[\text{DIC}]}{Q_a(\lambda)} = e^{-(m_1 + m_2(\lambda - 290))}, \quad (2)$$

where AQY is the apparent quantum yield ($[\text{DIC}]/Q_a(\lambda)$; $\text{mol DIC mol photons}^{-1}$), λ is wavelength (nm), and m_1 (dimensionless) and m_2 (“spectral slope coefficient”, nm^{-1}) are fit parameters, and:

$$\text{AQY}(\lambda) = \frac{[\text{DIC}]}{dQ_a(\lambda)} = ce^{-d\lambda}, \quad (3)$$

where c ($\text{mol DIC/mol photons}$, or dimensionless) and d (“spectral slope coefficient”, nm^{-1}) are fitting parameters. Details on parameter optimization and further method details are given in Supporting Information Table S1.

Given the substantial differences between the cut-off filter and the full-irradiance method to determine AQY spectra and the differences in spectral fitting between laboratories, we could not use a single statistical method to estimate uncertainty of the AQY fit parameters and confidence intervals on the AQY spectra across laboratories. In recent studies, uncertainty and confidence intervals were determined using bootstrapping (Groeneveld et al. 2016; Koehler et al. 2016) or Monte Carlo simulations (Gu et al. 2017), but confidence intervals determined with these differing methods across laboratories are not comparable. Therefore, we present in this study only the mean AQY spectra from replicate determinations at each laboratory without uncertainty estimates (Fig. 2). Differences in photochemical reactivity are compared using the wavelength-integrated AQY from 300 to 450 nm, denoted $\int_{300}^{450} \text{AQY}$. In addition to this comparison of experimentally determined AQY spectra, we also calculated the ratio of total photochemical DIC production under full solar simulated irradiance to the total DOM-absorbed photons integrated from 300 to 450 nm, denoted broadband $\overline{\text{AQY}}_{300-450}$. This second comparison ($\overline{\text{AQY}}_{300-450}$) is independent of the differing laboratory-specific spectral fitting approaches, and consequently integrates the combined effect of all other differences in method approach (Fig. 1) without the final determination of the AQY spectrum.

Chemical actinometry

The accuracy of each laboratory’s calculations of DOM-absorbed photons for use in AQY calculations was tested with ultraviolet actinometry by all groups except Jyväskylä. Here, the photon exposure of the irradiated actinometer solution was determined inside the sample containers used for irradiation experiments using the well-quantified photochemical production of hydroxyl radical from nitrite and its subsequent reaction with benzoic acid to form salicylic acid which was

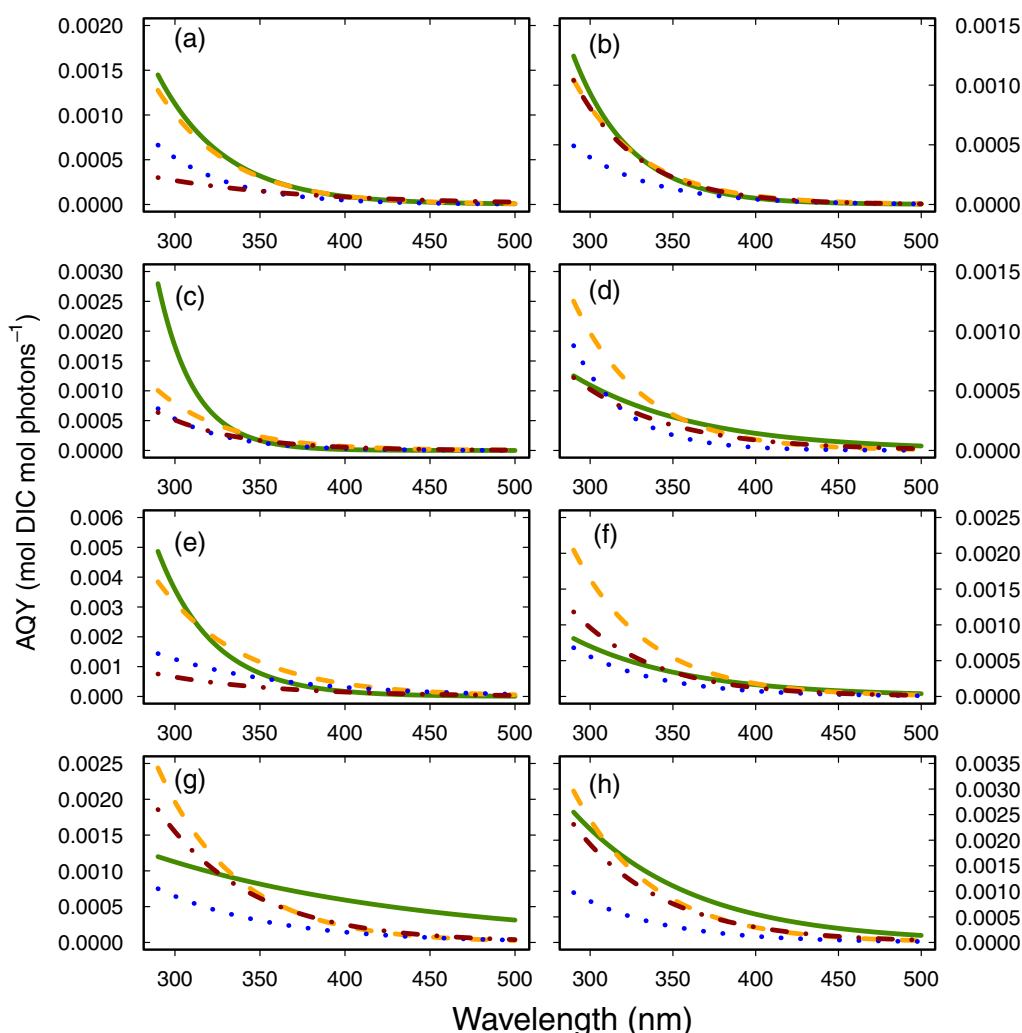


Fig. 2. AQY spectra for the photochemical production of DIC in water from eight inland waters, sorted by ascending concentrations of DOC (Table 1), with (a) Toolik Lake, (b) Norra Bredsjön, (c) Övre Skärsjön, (d) Jyväsjärvi, (e) Imnavait Creek, (f) Gäddtjärn, (g) Grästjärn, and (h) Svartjärn. The AQY spectra were independently measured in four laboratories, that is, Georgia (green solid line), Jyväskylä (orange dashed line), Michigan (blue dotted line) and Uppsala (red dash-dot line).

measured with fluorescence spectrophotometry (Horiba SPEX FluoroMax-4; Horiba Aqualog) (Jankowski et al. 1999, 2000). Each irradiation setup was verified to be compatible with the response bandwidth of the nitrite UV actinometer, designed specifically for use in sunlight, using spectral irradiance measurements of the light source and the absorbance spectrum of nitrite. The total radiant UV photon flux measured by actinometry inside sample cells was directly compared to calculations made using instrument-measured spectral irradiance outside the cell (Supporting Information Fig. S2) with geometrical and optical assumptions about pathlength over the same response bandwidth. Results are presented in Supporting Information Table S1.

Water chemistry

Additional chemical parameters were determined for water samples at the Uppsala Laboratory, with sub-samples taken

and analyzed just before starting the irradiation experiments (i.e., after storage and sample pretreatment). DOC concentrations were determined using high-temperature combustion (Shimadzu TOC-L; range of 4–30,000 ppm, detection limit of 4 ppb, CV of $\pm 1.5\%$ of max or 4 ppb) or wet chemical oxidation (Sievers 900; range of 0.03–50 ppm, precision of $< 1\%$ relative standard deviation and accuracy of 2% or 0.5 ppb, whichever is greater) each calibrated with potassium hydrogen phthalate standards. Total dissolved nitrogen and total dissolved phosphorus concentrations were determined on filtered lake water ($0.2 \mu\text{m}$ Supor®-200 membrane filters) as described in detail earlier (Groeneveld et al. 2016). For total dissolved iron analysis, a refiltered water sample was acidified with 0.5% concentrated nitric acid, and analyzed using an ICP-OES Optima 8300 (Perkin Elmer Life and Analytical Sciences).

UV-vis absorbance

UV-vis absorbance spectra were measured in 0.5- or 1-cm quartz cuvettes, just before starting the irradiation experiments, using spectrophotometers (Lambda models 35, 40 and 850, Perkin Elmer Life and Analytical Sciences, Waltham, Massachusetts, USA) or a spectrofluorometer (Aqualog, Horiba Scientific Instruments and Systems, Piscataway, New Jersey, USA). Based on the Beer-Lambert law, Napierian absorption coefficients, a_g (m^{-1}) were calculated as

$$a_g = \frac{A \ln 10}{L}, \quad (4)$$

where A is absorbance (dimensionless) and L is optical path length (m) (Kirk 1994). Integrated absorbance by chromophoric DOM was calculated in the range of 280–600 nm by applying trapezoidal integrations under the curve of a vs. wavelength (Moran et al. 2000). The slopes of the absorption spectrum between 275 and 295 nm ($S_{275-295}$) and between 350 and 400 nm ($S_{350-400}$) were calculated by linear regression to the natural logarithmically transformed data, and the slope ratio (S_R) was calculated as $S_{275-295}/S_{350-400}$ (Helms et al. 2008).

Photochemical rate modeling

For the five Swedish lakes (Table 1), we used the AQY spectra determined in each laboratory to simulate area-specific photochemical DIC production rates in the wavelength range 280–600 nm (1-nm resolution) from the surface of each lake in 0.005-m-increments down to the mean lake depth of the lakes included in the Swedish National Lake Inventory (3.9 m; Koehler et al. 2014), as

$$\Psi_{\text{DIC}}^{\text{Day}}(z) = \int_{\lambda_{\min}}^{\lambda_{\max}} E_{\text{od}}^{\text{Day}}(\lambda, 0^-) a_g(\lambda) e^{-(K_d(\lambda)z)} \Phi(\lambda) d\lambda, \quad (5)$$

where $\Psi_{\text{DIC}}^{\text{Day}}$ is daily DIC photoproduction ($\text{mol C m}^{-3} \text{ d}^{-1}$), z is depth (m), λ_{\min} and λ_{\max} are the minimal and maximal wavelengths (nm), $E_{\text{od}}^{\text{Day}}(\lambda, 0^-)$ is daily integrated downwelling scalar irradiation just below the water surface ($\text{mol photons m}^{-2} \text{ d}^{-1} \text{ nm}^{-1}$), a_g is the CDOM absorption coefficient (m^{-1}), K_d is the vertical attenuation coefficient for downward irradiance (m^{-1}), and $\Phi(\lambda)$ is the AQY of DIC photoproduction ($\text{mol C mol photons}^{-1}$). For each lake, daily integrated downwelling irradiation just below the water surface ($E_{\text{od}}^{\text{Day}}(\lambda, 0^-)$; $\text{mol photons m}^{-2} \text{ d}^{-1} \text{ nm}^{-1}$) was simulated for the autumnal equinox 2014 (22 September), as described in detail in Koehler et al. 2014. $a(\lambda)$ was measured, and $K_d(\lambda)$ was estimated using regression relationships with $a(\lambda)$ derived from literature data ($n = 565$) for nine wavelengths between 300 and 400 nm, with subsequent fitting of an exponential function to obtain continuous spectra (Koehler et al. 2014). $\Phi(\lambda)$ was measured for each lake in each of the four laboratories.

Statistical analyses

Differences in coefficients of variation for $\overline{\text{AQY}}_{300-450}$ and $\int_{300}^{450} \text{AQY}$, between laboratories and between lakes, were assessed using t -tests. Linear mixed-effects models were used to assess the influence (fixed effect) of “laboratory” (alternatively “lake”), on water chemical and optical parameters, as well as on $\overline{\text{AQY}}_{300-450}$ and $\int_{300}^{450} \text{AQY}$, defining “lake” (alternatively “laboratory”) as random effect, and assessing the significance of the fixed effect based on ANOVA (Crawley 2012). Linear mixed-effects models were also used to assess the influence (fixed effect) of water chemical and optical parameters on $\overline{\text{AQY}}_{300-450}$, defining the laboratory as random effect. The p -values were multiplicity adjusted using a single-step method (Hothorn et al. 2008). Linear least square regression analyses were used to describe relationships between $\overline{\text{AQY}}_{300-450}$ and the water chemical and optical parameters (see Table 1), and significance was assessed by regression ANOVA (Crawley 2012). Right-skewed variables were \log_{10} -transformed prior to analysis. In all analyses, differences were considered significant if p -value ≤ 0.05 . Mean values in the text are given with ± 1 standard error. Analyses were conducted using R 3.1.1 (R Development Core Team 2014) and Matlab® (R2014b). Throughout the text, variability between lake water samples for a given laboratory is referred to as “inter-water variability.” For variability between laboratories for a given water sample, we call this “inter-laboratory variability.”

Assessment

Inland water physical and chemical characteristics

The eight studied inland waters, situated in Alaska, Finland, and Sweden, are shallow systems with mean depths between < 1 and 7.3 m, and water retention times between ca. 2 weeks and 3.5 yr (Table 1). The inland waters also span a 5-fold range in DOC concentration and a nearly 10-fold range in DOM absorption coefficients, covering a large gradient from clear to brown-water systems (Table 1).

Across lakes, the pH values determined prior to the irradiation experiments did not differ between Georgia and Michigan laboratories ($p = 0.949$), but were lower in Jyväskylä and Uppsala laboratories (compared to the values measured in Georgia; both $p < 0.001$; Supporting Information Table S4). The CDOM values did not differ between Georgia and Jyväskylä laboratories ($p = 0.843$), while they were lower in Michigan and Uppsala laboratories (compared to Georgia; both $p < 0.002$; Supporting Information Table S4). The values of $a_g(420)$ measured at Georgia laboratory were similar to those measured at Jyväskylä and Uppsala laboratories (both $p > 0.253$), while $a_g(420)$ measured at Michigan laboratory was lower (compared to Georgia, $p = 0.0003$; Supporting Information Table S4). Finally, S_R was similar between all laboratories (Supporting Information Table S4, all $p > 0.605$). The inter-laboratory CV for these four parameters ranged from 3% to 20% (Table 1).

AQY spectra

The AQY spectra for DIC photoproduction determined in four laboratories varied by wavelength within each lake and between laboratories. There was no general pronounced bias with any of the laboratories which would give AQY spectra that consistently or strongly deviated from the inter-approach variability spanned in this study (Fig. 2). For example, for Imnavait Creek, the value of AQY determined at Georgia laboratory was largest at 300 nm, but fell below the AQY determined at Jyväskylä laboratory at ca. 325 nm (Fig. 2e). The higher AQY values determined for Imnavait Creek at the Michigan and Uppsala laboratories converged with the lower values determined at the Jyväskylä and Georgia laboratories at the visible range of the spectrum (Fig. 2e). The spectral variability in AQYs arises from the spectral slope coefficients of AQY, which overall ranged from 0.0064 to 0.0470 nm⁻¹ (Supporting Information Table S3). The normalized root mean squared error for linear regressions between DIC photoproduction measured in the irradiation experiments vs. predicted using the fitted AQY spectra varied between 5% and 19% across lakes and laboratories (Supporting Information Table S2, which also gives slopes and R^2 values of the linear regressions; see Supporting Information Table S3 for fitting parameters).

$\overline{\text{AQY}}_{300-450}$

The inter-laboratory variability in $\overline{\text{AQY}}_{300-450}$ (i.e., mean and SE of the determinations across laboratories) ranged from 0.14 ± 0.03 (mean \pm SE) mmol DIC mol photons⁻¹ (Övre Skärsjön) to 0.56 ± 0.14 mmol DIC mol photons⁻¹ (Imnavait Creek; Table 2). The inter-laboratory CV in $\overline{\text{AQY}}_{300-450}$ ranged from 33% to 49%, averaging $42\% \pm 2\%$ (Table 2; Supporting Information Table S4). This variability was smaller than the inter-water CV of $\overline{\text{AQY}}_{300-450}$ that ranged from 59% to 72%, averaging $65\% \pm 3\%$ ($p = 0.0002$, Table 2). For comparison, the mean intra-laboratory CV in $\overline{\text{AQY}}_{300-450}$, that is, for pseudo-replicate measurements in the same laboratory, ranged from 3% to 24%, and averaged 12% across the four laboratories (Supporting Information Table S5). Across lakes, $\overline{\text{AQY}}_{300-450}$ measured at Jyväskylä laboratory did not differ from that measured at Georgia laboratory ($p = 0.133$), while $\overline{\text{AQY}}_{300-450}$ measured at the Michigan and Uppsala laboratories were lower (compared to Georgia, both $p < 0.0033$; Supporting Information Table S5). Across laboratories, three lakes had similar $\overline{\text{AQY}}_{300-450}$ values compared to lake Gäddtjärn (Jyväsjärvi, Norra Bredsjön, and Toolik Lake; Supporting Information Table S5, all $p > 0.264$). One lake had lower $\overline{\text{AQY}}_{300-450}$ values (Övre Skärsjön, $p = 0.0402$), and the remaining three lakes had higher $\overline{\text{AQY}}_{300-450}$ values (Grästjärn, Imnavait Creek and Svartjärn, all $p < 0.001$; Supporting Information Table S5), again compared to Gäddtjärn.

$\int_{300}^{450} \text{AQY}$

The $\int_{300}^{450} \text{AQY}$ values ranged from 28 ± 4 mmol DIC mol photons⁻¹ (Norra Bredsjön) to 97 ± 21 mmol DIC mol photons⁻¹ (Table 2). The inter-laboratory CV of $\int_{300}^{450} \text{AQY}$ was similar to that for $\overline{\text{AQY}}_{300-450}$, averaging $38\% \pm 3\%$ (Table 2). The inter-water CV of $\int_{300}^{450} \text{AQY}$ ($63\% \pm 1\%$) was larger than the inter-laboratory variability ($p = 0.0001$, Table 2). Across lakes, the $\int_{300}^{450} \text{AQY}$ values measured at Jyväskylä laboratory did not differ statistically from those measured at Georgia laboratory ($p = 0.998$), while $\int_{300}^{450} \text{AQY}$ values measured at the Michigan and Uppsala laboratories were lower ($p < 0.0033$; Supporting Information Table S5). Across laboratories, three lakes had similar $\int_{300}^{450} \text{AQY}$ values compared to lake Gäddtjärn (Jyväsjärvi, Norra Bredsjön, and Toolik Lake; Supporting Information Table S5, all $p > 0.061$). One lake had lower $\int_{300}^{450} \text{AQY}$ values (Övre Skärsjön, $p = 0.0333$), and the remaining three lakes had higher $\int_{300}^{450} \text{AQY}$ values (Grästjärn, Imnavait Creek, and Svartjärn, all $p = 0.0246$; Supporting Information Table S5), again compared to Gäddtjärn.

$\overline{\text{AQY}}_{300-450}$ and water quality

Pooling the data from the four laboratories ($n = 32$), we found that $\log_{10}(\overline{\text{AQY}}_{300-450})$ was positively related to $a_g(420)$ ($R^2 = 0.31$, $p = 0.0003$), and negatively related to the slope ratio ($R^2 = 0.21$, $p = 0.0033$) and to pH ($R^2 = 0.16$, $p = 0.0007$). When testing these relationships separately per laboratory the trends were similar ($n = 8$; Supporting Information Fig. S1) but significant only for a subset of the datasets, specifically for $\overline{\text{AQY}}_{300-450}$ with $a_g(420)$ for Uppsala laboratory (Supporting Information Fig. S1a; $R^2 = 0.66$, $p = 0.0092$), with the slope ratio for Michigan laboratory (Supporting Information Fig. S1f; $R^2 = 0.43$, $p = 0.0467$) and with pH for Jyväskylä laboratory (Supporting Information Fig. S1k; $R^2 = 0.41$, $p = 0.0508$).

Simulated DIC photoproduction

For the five Swedish lakes in this study, DIC photoproduction was simulated, as detailed in Koehler et al. 2014, using modeled solar irradiances, measured sample CDOM absorption coefficients and the laboratory-specific measured AQY spectra. Thus, these simulations illustrate the variability in estimated photochemical DIC fluxes due to the variability in AQY spectra alone. Simulated DIC photoproduction rates ranged from 3.1 ± 0.5 mg C m⁻² d⁻¹ (Övre Skärsjön) to 26.2 ± 11.7 mg C m⁻² d⁻¹ (Grästjärn; Table 2). For three Swedish lakes (Gäddtjärn, Norra Bredsjön, Övre Skärsjön), the inter-laboratory variability of simulated DIC photoproduction ranged from a CV of 22% to 42% (Table 2). For Grästjärn (CV = 90%) and Svartjärn (CV = 60%), the inter-laboratory variability was much higher. Taken together, inter-laboratory differences in AQY spectra for these five lakes resulted in up to

Table 2. Mean (\pm SE), ratio of maximum to minimum and CV for the broadband AQY ($\overline{\text{AQY}}_{300-450}$, mmol DIC mol photons $^{-1}$), the wavelength-integrated AQY spectrum ($\int_{300}^{450}\text{AQY}$, mmol DIC mol photons $^{-1}$) and the simulated DIC photoproduction rates ($\text{mg C m}^{-2} \text{ d}^{-1}$) between lakes for each laboratory (upper part of the table) and between laboratories for each lake (lower part of the table).

	$\overline{\text{AQY}}_{300-450}$	Max/min	CV (%)	$\int_{300}^{450}\text{AQY}$	Max/min	CV (%)	Simulated DIC photoproduction	Max/min	CV (%)
Inter-water variability (n = 8)									
Georgia	0.45 ± 0.10	4.0	64.7	69.50 ± 15.63	4.4	63.6	25.04 ± 11.98	25.3	106.9
Jyväskylä	0.35 ± 0.08	5.3	64.5	71.12 ± 15.40	4.8	61.3	12.36 ± 3.64	5.4	65.8
Michigan	0.18 ± 0.05	5.3	72.1	32.53 ± 7.25	4.5	63.0	6.07 ± 1.70	4.7	62.6
Uppsala	0.24 ± 0.05	4.6	59.1	44.86 ± 10.00	5.1	63.0	11.57 ± 3.33	6.9	70.5
Mean \pm SE	0.48 ± 0.3		65.1 ± 2.7		4.7 ± 0.2	62.7 ± 0.5		10.6 ± 4.9	76.5 ± 10.3
Inter-laboratory variability (n = 4)									
Toolik Lake	0.18 ± 0.03	2.1	34.9	31.46 ± 6.59	2.3	41.9	NA	NA	NA
Norra Bredsjön	0.16 ± 0.03	2.4	33.2	28.34 ± 3.70	1.9	26.1	3.92 ± 0.43	1.7	21.7
Övre Skärsjön	0.14 ± 0.03	2.5	39.3	27.34 ± 4.24	2.0	31.0	3.12 ± 0.50	2.0	32.3
Jyväsjärvi	0.17 ± 0.03	2.7	37.1	30.57 ± 4.54	2.0	29.7	NA	NA	NA
Innavait Creek	0.56 ± 0.14	3.5	48.6	96.57 ± 24.30	3.9	50.3	NA	NA	NA
Gäddtjärn	0.23 ± 0.05	3.3	46.9	46.30 ± 9.32	2.7	40.3	9.11 ± 1.93	2.4	42.4
Grästjärn	0.47 ± 0.12	3.1	49.2	78.44 ± 14.69	2.8	37.5	26.19 ± 11.67	5.8	89.1
Svartjärn	0.53 ± 0.12	3.2	44.6	96.98 ± 20.98	3.5	43.3	25.74 ± 7.58	4.9	58.9
Mean \pm SE	0.29 ± 0.2		41.7 ± 2.3		2.6 ± 0.3	37.5 ± 2.9		3.4 ± 0.8	48.9 ± 11.8

between twofold and sixfold differences in simulated DIC photoproduction (max/min in Table 2).

Discussion

Inter-laboratory differences in AQY

The AQY spectrum is an essential, sensitive, yet poorly constrained model parameter for simulating DIC photoproduction in inland waters. This study shows the general magnitude of differences in AQY spectra, when methods and systems currently in use in a number of laboratories are applied as previously published (Cory et al. 2013; Powers and Miller 2015a; Groeneveld et al. 2016; Gu et al. 2017). This discussion first compares the inter-laboratory variability in AQY spectra to the analytical uncertainty within laboratory as well as to other inter-comparison studies concerning DOM, photochemistry, and water chemistry. The latter part of the discussion points out the main difficulties and challenges shared by all laboratories, with a tentative evaluation of their apparent importance in contributing to the observed inter-approach AQY differences.

Since we have no standard or “true” AQY spectrum against which we can validate our results we cannot quantify the deviation of our determined AQY spectra from an accurate photochemical reactivity spectrum for CDOM. The determination of AQY requires several analytical measurements (e.g., CDOM, spectral photon flux and at least two measurements of DIC concentration, Fig. 1) and the error of each analytical determination propagates in the resulting AQY. The uncertainty of AQY was 1%–40% (median 13%) for individual water samples when the propagation of error in analytical precision for determination of DIC, CDOM, and photon fluxes was accounted for in one laboratory (Aarnos et al. 2012, 2018). Broadband AQY values for the photochemical production of singlet oxygen from the standard reference material Suwannee River Fulvic Acid (SRFA) ranged from 0.004 to 0.031 with a CV of 38% when results from 11 studies were compared (Ossola et al. 2021). Therefore, our observed 30–50% inter-laboratory variability in $\overline{\text{AQY}}_{300-450}$ and $\int_{300}^{450} \text{AQY}$ values (Table 2) is not surprising and may indeed be seen as an encouragingly good end-result for such a complex method where the approaches were purposely not standardized between laboratories prior to the study. Confidence in the method is also gained from the fact that we found similar trends of $\overline{\text{AQY}}_{300-450}$ with water chemical and optical properties across laboratories (Supporting Information Fig. S1, though only significant in 25% of the cases for the small sample size of $n = 8$ per regression), and that the respective relationships were significant when pooling the data across laboratories ($n = 32$, and using lme-models to account for the fact that samples per lake were not independent between laboratories).

To further put our observed inter-laboratory variability in perspective, given that there are no previous inter-comparison studies on DIC photoproduction rates, let alone DIC AQY spectra, we compared our results with other inter-comparison studies for various analytes in natural waters. An earlier marine inter-comparison of DOC concentrations found agreement within 7.5% between four laboratories, but differences were much larger in two other laboratories (Sharp et al. 1995). The variability between 20 laboratories in determining DOM fluorescence of well-determined fluorophores and natural waters typically ranged from 10% to 15% for several humic-like peaks, and from 15% to 35% for two protein-like peaks (Murphy et al. 2010). A large-scale inter-comparison for dissolved iron concentrations in seawater had a CV of 36% between 24 laboratories (Bowie et al. 2006). Again, now in the context of these earlier inter-comparison studies, we conclude that the observed 30–50% CV in DIC AQY is an encouragingly good inter-laboratory agreement. This conclusion is further strengthened by the fact that AQY determination requires several independent analytical measurements, with respective propagation of errors to the final result.

The inter-laboratory uncertainty in the DIC AQY spectra demonstrated here should be considered when working with DIC AQY results, comparisons, and modeling. In the sections below, we illustrate current knowledge gaps and the best practices moving forward in both our understanding of the specific causes of variability in determined DIC AQY spectra and our ability to make best estimates for DIC AQY. Further reducing inter-laboratory variability could considerably reduce uncertainty in photochemical modeling.

Considerations for sample handling and treatment

For our comparison, we assumed that the samples analyzed in each laboratory from each water had the same photochemical reactivity and AQY spectra at the time of measurement in each of the four laboratories. However, the water samples experienced different storage times in each laboratory before analysis (i.e., 1 week to 5 months storage of filtered water in the dark at 4°C; Supporting Information Table S1). A certain time of cold sample storage before AQY measurements is common, but may modify the DOM of the water samples. For instance, both DOC concentrations and DOM absorbance degraded during cold storage of filtered peatland samples with relatively high initial DOC concentrations (~ 5 to $> 50 \text{ mg C L}^{-1}$), showing an average loss of 5% DOC in 3 months storage time (Peacock et al. 2015). These changes may occur quite rapidly, as already 1 week of cold storage modified lake water DOC concentrations and fluorescence properties (Heinz and Zak 2018). Such storage effect may explain why absorbance (i.e., $a_g(420)$ and integrated CDOM values), measured following storage but before the irradiation experiments, showed statistically significant differences between some laboratories (inter-laboratory CV of 3–20%, Table 1). This interpretation is

consistent with the fact that CDOM measured at the two laboratories with the longest storage times (i.e., Michigan and Uppsala) was somewhat lower prior to irradiation than CDOM in the laboratories with considerably shorter storage times (Supporting Information Table S1), and with the observation of flocculant material in some water samples after preexperiment storage in Michigan laboratory. This implies that storage effects likely contributed to the observed differences in AQY spectra (inter-laboratory CV of 33–49%, Table 2).

Although freezing is often used to preserve samples for DOC analysis, freeze/thaw can cause DOC loss by flocculation and large changes in sample optical properties (Fellman et al. 2008; Peacock et al. 2015; Heinz and Zak 2018) and is therefore not recommended for DIC and any CDOM-based photochemistry experiments. Most laboratory irradiation setups are not field portable and typically only allow one AQY experiment to be completed per day, often making it impossible to analyze comparative samples within 24 h of collection. An evaluation of changes in DIC photoproduction rates due to storage would be beneficial, but this type of assessment is still missing from the literature. Consequently, for inland waters with high DOC concentrations, DIC photoproduction experiments on both freshly collected and stored samples are needed to better understand the variability in measured rates arising from storage artifacts alone. Meanwhile, keeping storage times prior to irradiation as short as possible is recommended to reduce the potential storage effect on the resulting AQY spectra. An alternative approach to minimize sample storage artifacts is to adopt newly developed, portable, and high-throughput LED-based methods (Bowen et al. 2020; Ward et al. 2021).

Analytical and chemical considerations

DIC-stripping by acidification and rebuffering of the water sample is often used to reduce background DIC concentrations prior to irradiation, as was done in several laboratories in this study too (Supporting Information Table S1). Specifically, no sample pretreatment was conducted at the University of Michigan laboratory, while all other laboratories acidified samples to $\text{pH} < 3$ using concentrated hydrochloric acid, bubbled using CO_2 -free air or nitrogen gas for 30–60 min, and used sodium borate or sodium hydroxide to readjust each sample to its original pH. In an earlier assessment, this DIC removal step caused an increase in UV-B absorbance of about 5% but did not affect absorbance at longer wavelengths (Johannessen and Miller 2001). Furthermore, photoproduced DIC agreed during early stages of irradiation (< 2 h) between natural river water and water that had been acidified, DIC-stripped, and rebuffered, but for one water sample that was irradiated for 14 h the DIC-stripped treatment gave DIC photoproduction that was ca. three times lower than for the unamended treatment (Powers et al. 2017b). Also, the mathematical fitting parameters for the DIC AQY spectra of three Swedish low-DIC

lakes did not differ between DIC-stripped and non-stripped water samples (Koehler et al. 2016). These studies suggest only a minor effect of this sample pretreatment on photochemical reactivity, at least for the tested conditions.

However, particularly in waters with low alkalinity, it can be challenging to restore the exact pH of the original sample in a stable way. Furthermore, the choice of buffer (e.g., sodium borate) or sodium hydroxide (unbuffered) will affect the buffering capacity of the sample, and therefore how much pH changes during irradiation. Potential artifacts from pH manipulations of this kind include DOC moieties that precipitate or form colloids at low pH resisting redissolution, and changes in trace metal speciation relevant to photochemical pathways. Although pH is often lowered to below pH 3, a pH of 4 should be adequate to remove background DIC and potentially preserve DOM quality. Nonetheless, further systematic testing is required to better understand effects of DIC-stripping on sample integrity. Until new methods become available that allow reliable, sensitive analysis of photo-produced DIC with minimal sample manipulation, we are limited by experimental methods that reduce DIC background and generate a DIC signal large enough to accurately quantify photo-oxidation by using high-intensity radiation of typically several hours duration. Recent methods based on stable carbon isotope changes in the sample DIC pool during irradiation experiments may help lower the detection limit of DOM photooxidation and overcome sample pretreatment (Wang et al. 2009; Powers et al. 2017a, 2017b).

Regardless of these potential effects, there were preirradiation differences in pH that were measured following storage but before irradiation between some laboratories (interlaboratory CV of 3–13%, Table 1). This variability could be due to differences in sample handling, pretreatment methods (filtration with or without DIC-stripping and rebuffering) and storage, as well as in the methods used to determine sample pH, and consequently added to the inter-laboratory variability of the determined AQY. Specifically, iron is known to enhance DIC photoproduction rates (Gao and Zepp 1998; Xie et al. 2004; Gu et al. 2017; Bowen et al. 2020). Hence, differences in sample storage, sample treatment, and pH mentioned above could have changed iron speciation and concentration, and therefore influenced CDOM absorption (Xiao et al. 2013) and DIC photochemistry (Xie et al. 2004; Gu et al. 2017) in this study.

It is also important to consider that pH values can change considerably in unbuffered samples during photochemical irradiations (Xie et al. 2004; Timko et al. 2015). For example, pH decreased by 1.4–1.8 units over a >24 h irradiations of river water samples, and the largest pH loss occurred during the early stages of the irradiation (Xie et al. 2004). Irradiation time and sample conditions (i.e., buffered or unbuffered) and therefore absorbed photon doses varied widely between laboratories and samples (Supporting Information Table S1), suggesting that sample pH during irradiation has likely also varied between laboratories. Since pH values are critical to consider

during most photochemical experiments, monitoring pH over the time course of irradiation could help quantify its influence on DIC photoproduction rates, particularly in freshwater samples. Efforts have been made to control sample pH during irradiation experiments using a micro pH electrode and μL additions of acid and base (Timko et al. 2015), but these systems have yet to be developed for the irradiation setups required for AQY determinations. Furthermore, given that glass pH electrodes may require long equilibration times in these natural freshwaters (Stauffer 1990) and are prone to large drift over time scales of irradiation experiments, it is uncertain if use of a similar system would help in this regard. Often, buffers (e.g., sodium borate as used by some here) are used to stabilize sample pH but there is a lack of “real-time” evaluations of their ability to control sample pH during irradiations, and they remain largely untested for their potential impacts on DIC photoproduction rates. Assessments of the effect of specific buffers on the determination of DIC AQY spectra may help explain and reduce the observed inter-laboratory differences.

Considerations for irradiation designs and subsequent AQY determination

The inter-laboratory differences were similarly large in both the broadband AQY ($\overline{\text{AQY}}_{300-450}$) and the wavelength-integrated AQY ($\int_{300}^{450} \text{AQY}$). By design, the differences in $\overline{\text{AQY}}_{300-450}$ do not reflect differences in spectral fitting routines between laboratories (Supporting Information Table S1). As discussed above, while it is likely that sample handling and storage contributed to the differences observed here, the inter-laboratory differences in $\overline{\text{AQY}}_{300-450}$ were considerably larger (CV of 33–49%, Table 2) than in the preirradiation water optical properties and pH (CV of 3–20%, Table 1). Also, the average intra-laboratory CV in $\overline{\text{AQY}}_{300-450}$ (12%, based on Supporting Information Table S5) was considerably smaller than the average inter-laboratory CV (42%, Table 2). This suggests that part of the inter-laboratory differences resulted from difficulties in determining adequate (1) photochemical DIC production and (2) DOM-absorbed photons from the irradiation setups and experiments, that is, apart from the purely analytical aspects.

Difficulties concerning point (1) include evidence that DIC photochemical efficiency decreases as photon dose increases (Miller and Zepp 1995; Powers and Miller 2015a). This means that the sampling intervals for DIC analysis can significantly affect results, and the linear assumption made to determine DIC production rates for AQY calculations, even when corrected for photochemical bleaching of CDOM, is only valid over short irradiation intervals (Miller and Zepp 1995; Powers and Miller 2015a). In this study, inter-laboratory and inter-water irradiation times and photon doses were variable (Supporting Information Table S1). Unfortunately, quantifying DIC photoproduction after very short exposure is often

not possible due to the small light vs. dark differences in DIC, particularly against a large DIC background concentration (i.e., in unsparged samples). Moreover, very few studies that use methods similar to the ones described here have reported detection limits for photoproduced DIC, more often reporting data for ultrapure water blanks (Johannessen and Miller 2001; White et al. 2008) or as the difference in DIC concentrations in the dark controls before and after the irradiation experiment. Until new methods with higher accuracy and precision become available for determination of DIC photoproduction rates (Powers et al. 2016), DIC AQY spectra will continue to be determined from light exposures that last long enough to achieve the minimum DIC needed to detect a light vs. dark difference in DIC concentration.

An accurate AQY should be compatible with rates that reproduce in situ DIC photoproduction. Therefore, it is important that laboratory experiments attempt to determine initial rates (Cory and Kling 2018), unless the aim is to describe, for example, DIC photoproduction rates from CDOM over its entire lifetime up to complete photobleaching (Aarnos et al. 2018). Therefore, it is important to choose irradiation times that are as short as possible to represent photochemical production of DIC, particularly for inland waters where photochemical removal of reactive CDOM may be continually replenished (Cory et al. 2015; Cory and Kling 2018). Another aspect to consider in this context is that, in the case of a freshwater lens or in highly stratified systems in summer, photobleaching in situ may be faster than mixing. Due to the polychromatic nature of sunlight and both direct and indirect bleaching effects CDOM photobleaching is not trivial to model. A new method which determines an AQY matrix for CDOM photobleaching has recently been developed, and it was demonstrated that temperature and prior exposure history had a large influence on the magnitude and spectral shape of the CDOM photobleaching AQY matrix (Zhu et al. 2020). Ideally, determination of DIC photoproduction over the time course of exposure for a variety of samples is needed to better understand the impact of photon dose and light-absorbed by CDOM on the AQY, and to account for changes in the AQY spectrum in photochemical modeling where rates are scaled over time (see Vähatalo and Wetzel 2004). However, because DOM in situ is a complex mixture of likely various exposure histories, it is difficult to tease these differences out experimentally. Thus, as mentioned above, AQYs determined from initial rates in the laboratory give the best representation of environmental photochemical rates at the time of sampling from this complex DOM mixture.

Moreover, it is well known that DOM optical properties change as irradiation continues, altering the magnitude and spectral shape of absorbance (Del Vecchio and Blough 2002; Helms et al. 2008). Given that AQY depends on DOM photon absorption, changes in DIC photochemical efficiency might be expected to result from these changes in DOM absorbance properties. However, additional factors may also contribute to

the decline of DIC AQY over time. For example, oxygen (O_2) concentrations decrease during irradiations in sealed vessels (Gao and Zepp 1998; Xie et al. 2004; Cory et al. 2014), and DIC photoproduction has been noted to be highest in O_2 -saturated samples and lowest in nitrogen-saturated samples (Xie et al. 2004). Presumably, all water samples in our study were air-saturated prior to the irradiation experiments but since all experiments were conducted in sealed containers with no head-space, decreases in O_2 during the several hours long irradiations have the potential to decrease overall DIC photoproduction rates. While further factors other than oxygen concentration may be involved (e.g., dose dependence, see above), a_g -normalized DIC photoproduction rates in a tidal creek decreased from 300 nM m h^{-1} over the first 6 h of irradiation to 100 nM m h^{-1} after 48 h irradiation (Powers and Miller 2015b). Assuming a 1 : 1 ratio between CO_2 production and O_2 loss (see supporting information of Cory et al. 2014; also see Andrews et al. 2000, Bowen et al. 2020, Ward and Corry 2020), O_2 loss rates normalized to CDOM absorption would also decrease in a similar fashion, implying decreasing O_2 AQY values over time. The 1 : 1 assumption would imply a consumption of only $\sim 30 \mu\text{M } O_2$ in 48 h, and it is unknown whether this $\sim 15\%$ loss in O_2 is enough to impact DIC photoproduction rates. Although photochemical AQY spectra for photochemical O_2 consumption have been determined (Andrews et al. 2000; Cory et al. 2014; Ward et al. 2021), work is needed to determine how AQY spectra (for both O_2 loss and DIC production) vary at various O_2 concentrations to predict how these processes may change over the course of exposure. This uncertainty again demonstrates that it is important to aim for the shortest irradiation time possible that still allows for reliable DIC determination, and that the development of new methods, where DIC photoproduction can be determined over very short time scales, thus minimizing photochemical O_2 loss, will also help in this regard (Bowen et al. 2020; Ward et al. 2021).

Another inter-laboratory difference is that irradiation temperatures varied between 15°C and 30°C . An Arrhenius temperature dependence has been demonstrated for H_2O_2 AQY spectra, which is expected because H_2O_2 is a thermal product of superoxide decay (Kieber et al. 2014). Also, a similar temperature dependence of CO AQY spectra has been demonstrated (Zhang et al. 2006; Ren et al. 2014), albeit with lower activation energies than H_2O_2 . An Arrhenius equation was used to explain differences between laboratory DIC photoproduction rates and those measured in situ (Aarnos et al. 2012) and subsequent work showed that DOC loss was greater at higher temperature ($23\text{--}25^\circ\text{C}$) than lower temperature ($9\text{--}14^\circ\text{C}$) (Porcal et al. 2015), potentially indicating that DIC AQY spectra could also have an Arrhenius temperature dependence. Although all samples are “sterile-filtered,” bacterial regrowth remains possible, especially in the dark controls and in samples exposed to lower-energy visible light. In addition,

photochemical reactions produce low-molecular-mass organic compounds suitable for a rapid microbial mineralization to CO_2 . The irradiated samples should therefore be analyzed for DIC immediately after irradiation or stored only over a short time, for example, in an ice bath to minimize bacterial respiration. All laboratories took measures to minimize bacterial regrowth but, if present, it may pose a larger problem at higher temperatures or longer exposure times with respiration “contaminating” the measured DIC values in both irradiated samples and dark controls. It is encouraging that bacterial production was negligible in 0.2 to $0.7 \mu\text{m}$ filtered Toolik Lake dark controls (Ward et al. 2017) and that bacterial densities were negligible in samples kept in the dark and irradiated at 5°C under simulated solar radiation (Aarnos et al. 2012).

At higher irradiation temperatures, it may be tempting to control microbial regrowth with the use of bactericides such as NaN_3 , $ZnCl_2$ or $HgCl_2$. However, even if minor compared to the various potential matrix effects listed above, there is potential for bactericide participation in photochemical reactions. For instance, the very strong binding of Hg with DOM (Ravichandran 2004) and potentially its binding with carboxylic functional groups (Haitzer et al. 2003) may create unnatural photochemical pathways with unknown impact for DIC AQY spectra. Thus, while it is important to test the Arrhenius temperature dependence of DIC AQY spectra, microbial counts might also help to evaluate possible contamination in DIC determinations. Above all else, multiple dark controls should be measured in any AQY measurement to assess possible non-photochemical changes in DIC.

The accuracy of quantifying DOM-absorbed photons, point (2) above, is also a critical consideration when examining observed inter-laboratory differences in calculated $\overline{AQY}_{300-450}$. Even though photon absorption by CDOM is essential for any AQY method, equations used to describe CDOM-absorbed photons are often unclear or not described in the literature (e.g., examples in Hu et al. 2002). For the three laboratories that reported CDOM absorption by actinometry, the respective photon flux differed by $18\text{--}43\%$ from the calculated photon flux (Supporting Information Table S1). Although there are inherent errors in the application of chemical actinometry that could account for some of these differences, this result suggests that the calculations of CDOM-absorbed photons and underlying assumptions (i.e., the basic setup of the irradiation system including the simulator and vessels) likely contribute a significant share to the overall observed inter-laboratory differences for $\overline{AQY}_{300-450}$. Furthermore, the nitrite actinometer is optically thin (i.e., absorption coefficient \times pathlength $\ll 1$), but given the very high CDOM absorbance values for our study waters (Table 1), this actinometer may not best represent the samples during irradiation. In addition, the inter-laboratory differences in irradiation designs, and therefore optical pathlengths (Supporting Information Table S1), likely resulted in differences in the degree of shelf-shading. Diluting

samples is one option to ensure that samples have similar optical transparencies, but dilutions can also cause changes in solution chemistry, and decrease DIC photoproduction rates with the disadvantage that longer irradiation times would be required. Therefore, instead of dilution, the methods of Hu et al. (2002) (Eq. 1) were applied to correct the calculated DOM-absorbed photons for self-shading during irradiations. It is difficult, however, to test if this correction was complete, and consequently differences in self-shading might also have contributed to differences in determined DIC AQYs. In support of that interpretation, when solutions of Suwannee River natural organic matter representing a variety of DOC concentrations (1–18 mg C L⁻¹) were irradiated under optically thin conditions (1 mm flow cell), CDOM absorbance and fluorescence loss was significantly faster for the most dilute samples (1–3 mg C L⁻¹) (Armstrong et al. 2021). These results implied that samples at higher concentrations still experienced self-shading, despite the generally used criteria “absorption coefficient \times pathlength $\ll 1$ ” (Hu et al. 2002), or that there is another, not yet understood explanation for the concentration dependence of CDOM photobleaching. Regardless, given that much work is needed to resolve these issues, researchers should perform chemical actinometry with AQY measurements (Hu et al. 2002), a procedure that so far remains uncommon. At the least, chemical actinometry should be routinely used to test and verify the calculations of DOM-absorbed photons when an irradiation system is initially set up or changed, making sure that the general assumptions made during calculations are met (Ward et al. 2021).

In addition to these analytical and optical challenges, AQY spectra contain further uncertainty caused by commonly made assumptions regarding specific spectral mathematical fitting routines. Since not all used mathematical approaches can be applied for all formats of data obtained in the differing experimental approaches, we did not standardize the mathematical methods that currently differ substantially between laboratories (Fig. 1, Table S1). Differences include (1) mathematical fitting methods and how the AQY spectrum is constrained (i.e., a priori assumptions of spectral shape, number of measurements and optical treatments included in the fit, and choice of the starting values for the fitting routine); (2) the type of chemical and optical data (i.e., fitting actual measured data or derived data as is done in the so-called “difference method”; Rundel 1983); and (3) the methods used to evaluate the statistical uncertainty of the AQY spectra (currently bootstrapping or Monte Carlo simulations). The different choices made for mathematical fitting methods, data constraints, assumptions, and uncertainty assessment are partly dependent on the data format that results from the chosen experimental method approaches. Reaching a consensus on the optimal mathematical approaches for spectral AQY fitting and uncertainty assessment would require a previous consensus on the

optimal experimental approach/data format, which is not currently reached. A rigorous evaluation of the number of replicates and spectral treatments that gives a unique mathematical AQY spectral solution is needed to further assess and decrease the uncertainty among our groups’ AQY spectra caused by data handling and mathematical methods.

Conclusions

In summary, determining the AQY for the photochemical oxidation of DOM from inland waters is an undertaking that presents a common set of methodological challenges to all laboratories working on this problem. In this study, we purposely did not standardize or control for the many potential effects of the methodological choices on the resulting AQY spectra (e.g., storage time, pH adjustments, sample temperature, irradiation setups, number of replicate samples; Fig. 1; Supporting Information Table S1). The results of this study provide some constraints on the level of reproducibility currently obtained across different laboratories and serve as justification to work toward agreeing on a relatively more standardized protocol for AQY spectral measurements. Due to the different types of challenges inherent to different waters (e.g., low vs. high CDOM, low vs. high background DIC, low vs. high iron, wide range in pH), achieving one standard protocol for all waters may not be realistic. Rather, the results from this study should help raise awareness of the many methodological factors that may influence the AQY results.

Given the many potential sources of uncertainty and error in each of the sampling and method steps discussed here (Fig. 1) that may propagate in AQY calculations, we expected differences in AQY spectra of a given water sample measured across laboratories. It is encouraging that the inter-laboratory variability that we found in the DIC AQY spectra was much less than the inter-water variability (Table 2), with inter-laboratory differences similar to the uncertainty found for other challenging methods (e.g., iron, Bowie et al. 2006 or fluorescence, Murphy et al. 2010). An average inter-laboratory CV for AQY of ca. 40% (Table 2) is, especially given that there were no forced procedural directives, positive for such an advanced technical undertaking involving complex environmental samples and experimental decisions that include laboratory and environmental optics, chemistry and photochemical measurements, as well as mathematical and modeling expertise. This work should encourage more researchers to carry out AQY determinations, including methodological development and testing, and learn from our current mistakes and best practices.

Using photochemical rate modeling we found that the inter-laboratory differences in AQY spectra caused on average a 49% CV in the simulated photochemical DIC production for the five strongly differing Swedish lakes in this study (ranging from 22% to 89%, Table 2), and that the estimates were not consistently biased toward higher or lower rates between laboratories (Supporting Information Table S5). This variability does not alter conclusions on the relative importance of photochemical CO₂

production in inland waters (Cory et al. 2014; Koehler et al. 2014; Vachon et al. 2016). Using single AQY spectra from single systems for large-scale simulations, without awareness of the complexity of the measurements and uncertainty and sensitivity analyses, are discouraged. In situ data of DIC photo-production rates over water depth can be valuable for validation of photochemical rate models (Vähätalo et al. 2000; Koehler et al. 2014; Groeneveld et al. 2016). This is unfortunately rarely done but equally important in photochemical simulations as in other modeling exercises, and hence encouraged for future studies. It is important to consider the magnitude of inter-laboratory differences reported here when compiling or comparing AQY spectra between ecosystems, and when using the AQY spectra in photochemical rate models and interpreting the model output, especially for large-scale simulation studies and upscaling.

Data availability statement

The main raw data are available in the Supporting information. Remaining data and model code are available upon request from B. Koehler.

References

- Aarnos, H., Y. Gélinas, V. Kasurinen, Y. Gu, V. M. Puupponen, and A. V. Vähätalo. 2018. Photochemical mineralization of terrigenous DOC to dissolved inorganic carbon in ocean. *Global Biogeochem. Cycl.* **32**: 250–266. doi:[10.1002/2017GB005698](https://doi.org/10.1002/2017GB005698)
- Aarnos, H., P. Ylöstalo, and A. V. Vähätalo. 2012. Seasonal phototransformation of dissolved organic matter to ammonium, dissolved inorganic carbon, and labile substrates supporting bacterial biomass across the Baltic Sea. *J. Geophys. Res.* **117**: G01004. doi:[10.1029/2010JG001633](https://doi.org/10.1029/2010JG001633)
- Alleson, L., B. Koehler, J. E. Thrane, T. Andersen, and D. O. Hessen. 2021. The role of photomineralization for CO₂ emissions in boreal lakes along a gradient of dissolved organic matter. *Limnol. Oceanogr.* **66**: 158–170. doi:[10.1002/lno.11594](https://doi.org/10.1002/lno.11594)
- Andrews, S. S., S. Caron, and O. C. Zafiriou. 2000. Photochemical oxygen consumption in marine waters: A major sink for colored dissolved organic matter? *Limnol. Oceanogr.* **45**: 267–277. doi:[10.4319/lo.2000.45.2.0267](https://doi.org/10.4319/lo.2000.45.2.0267)
- Armstrong, A. W., L. Powers, and M. Gonsior. 2021. Reproducible determination of dissolved organic matter photosensitivity. *Biogeosciences* **18**: 3367–3390. doi:[10.5194/bg-18-3367-2021](https://doi.org/10.5194/bg-18-3367-2021)
- Belanger, S., H. Xie, N. Krotkov, P. Larouche, W. F. Vincent, and M. Babin. 2006. Photomineralization of terrigenous dissolved organic matter in Arctic coastal waters from 1979 to 2003: Interannual variability and implications of climate change. *Global Biogeochem. Cycl.* **20**: GB4005. doi:[10.1029/2006GB002708](https://doi.org/10.1029/2006GB002708)
- Bowen, J. C., C. P. Ward, G. W. Kling, and R. M. Cory. 2020. Arctic amplification of global warming strengthened by sunlight oxidation of permafrost carbon to CO₂. *Geophys. Res. Lett.* **47**: e2020GL087085. doi:[10.1029/2020GL087085](https://doi.org/10.1029/2020GL087085)
- Bowie, A. R., E. P. Achterberg, P. L. Croot, H. J. W. de Baar, P. Laan, J. W. Moffett, S. Ussher, and P. J. Worsfold. 2006. A community-wide intercomparison exercise for the determination of dissolved iron in seawater. *Mar. Chem.* **98**: 81–99. doi:[10.1016/j.marchem.2005.07.002](https://doi.org/10.1016/j.marchem.2005.07.002)
- Cole, J. J., and others. 2007. Plumbing the global carbon cycle: Integrating inland waters into the terrestrial carbon budget. *Ecosystems* **10**: 172–185. doi:[10.1007/s10021-006-9013-8](https://doi.org/10.1007/s10021-006-9013-8)
- Cory, R., K. Harrold, B. Neilson, and G. Kling. 2015. Controls on dissolved organic matter (DOM) degradation in a headwater stream: the influence of photochemical and hydrological conditions in determining light-limitation or substrate-limitation of photo-degradation. *Biogeosciences* **12**: 6669–6685. doi:[10.5194/bg-12-6669-2015](https://doi.org/10.5194/bg-12-6669-2015)
- Cory, R. M., B. C. Crump, J. A. Dobkowski, and G. W. Kling. 2013. Surface exposure to sunlight stimulates CO₂ release from permafrost soil carbon in the Arctic. *Proc. Natl. Acad. Sci.* **110**: 3429–3434. doi:[10.1073/pnas.1214104110](https://doi.org/10.1073/pnas.1214104110)
- Cory, R. M., and G. W. Kling. 2018. Interactions between sunlight and microorganisms influence dissolved organic matter degradation along the aquatic continuum. *Limnol. Oceanogr. Lett.* **3**: 102–116. doi:[10.1002/lo2.10060](https://doi.org/10.1002/lo2.10060)
- Cory, R. M., C. P. Ward, B. C. Crump, and G. W. Kling. 2014. Sunlight controls water column processing of carbon in arctic fresh waters. *Science* **345**: 925–928. doi:[10.1126/science.1253119](https://doi.org/10.1126/science.1253119)
- Crawley, M. J. 2012. *The R book*, 2nd Edition. John Wiley & Sons.
- Cullen, J. J., and P. J. Neale. 1994. Ultraviolet radiation, ozone depletion, and marine photosynthesis. *Photosynth. Res.* **39**: 303–320. doi:[10.1007/BF00014589](https://doi.org/10.1007/BF00014589)
- Del Vecchio, R., and N. V. Blough. 2002. Photobleaching of chromophoric dissolved organic matter in natural waters: Kinetics and modeling. *Mar. Chem.* **78**: 231–253. doi:[10.1016/S0304-4203\(02\)00036-1](https://doi.org/10.1016/S0304-4203(02)00036-1)
- Drake, T. W., P. A. Raymond, and R. G. Spencer. 2018. Terrestrial carbon inputs to inland waters: A current synthesis of estimates and uncertainty. *Limnol. Oceanogr. Lett.* **3**: 132–142. doi:[10.1002/lo2.10055](https://doi.org/10.1002/lo2.10055)
- Fellman, J. B., D. V. D'Amore, and E. Hood. 2008. An evaluation of freezing as a preservation technique for analyzing dissolved organic C, N and P in surface water samples. *Sci. Total Environ.* **392**: 305–312.
- Fichot, C. G., and W. L. Miller. 2010. An approach to quantify depth-resolved marine photochemical fluxes using remote sensing: Application to carbon monoxide (CO) photoproduction. *Remote Sens. Environ.* **114**: 1363–1377. doi:[10.1016/j.rse.2010.01.019](https://doi.org/10.1016/j.rse.2010.01.019)
- Gao, H., and R. G. Zepp. 1998. Factors influencing photoreactions of dissolved organic matter in a coastal river of the southeastern United States. *Environ. Sci. Technol.* **32**: 2940–2946. doi:[10.1021/es9803660](https://doi.org/10.1021/es9803660)

- Granéli, W., M. Lindell, and L. Tranvik. 1996. Photo-oxidative production of dissolved inorganic carbon in lakes of different humic content. *Limnol. Oceanogr.* **41**: 698–706. doi:[10.4319/lo.1996.41.4.0698](https://doi.org/10.4319/lo.1996.41.4.0698)
- Groeneveld, M., L. J. Tranvik, S. Natchimuthua, and B. Koehler. 2016. Photochemical mineralisation in a boreal brown water lake: Considerable temporal variability and minor contribution to carbon dioxide production. *Biogeosciences* **13**: 3931–3943. doi:[10.5194/bg-13-3931-2016](https://doi.org/10.5194/bg-13-3931-2016)
- Gu, Y., A. Lensu, S. Perämäki, A. Ojala, and A. V. Vähätalo. 2017. Iron and pH regulating the photochemical mineralization of dissolved organic carbon. *ACS Omega* **2**: 1905–1914. doi:[10.1021/acsomega.7b00453](https://doi.org/10.1021/acsomega.7b00453)
- Haitzer, M., G. R. Aiken, and J. N. Ryan. 2003. Binding of mercury (II) to aquatic humic substances: Influence of pH and source of humic substances. *Environ. Sci. Technol.* **37**: 2436–2441. doi:[10.1021/es026291o](https://doi.org/10.1021/es026291o)
- Heinz, M., and D. Zak. 2018. Storage effects on quantity and composition of dissolved organic carbon and nitrogen of lake water, leaf leachate and peat soil water. *Water Res.* **130**: 98–104. doi:[10.1016/j.watres.2017.11.053](https://doi.org/10.1016/j.watres.2017.11.053)
- Helms, J. R., A. Stubbins, J. D. Ritchie, E. C. Minor, D. J. Kieber, and K. Mopper. 2008. Absorption spectral slopes and slope ratios as indicators of molecular weight, source, and photobleaching of chromophoric dissolved organic matter. *Limnol. Oceanogr.* **53**: 955–969. doi:[10.4319/lo.2008.53.3.0955](https://doi.org/10.4319/lo.2008.53.3.0955)
- Hothorn, T., F. Bretz, and P. Westfall. 2008. Simultaneous inference in general parametric models. *Biom. J.* **50**: 346–363. doi:[10.1002/bimj.200810425](https://doi.org/10.1002/bimj.200810425)
- Hu, C., F. E. Muller-Karger, and R. G. Zepp. 2002. Absorbance, absorption coefficient, and apparent quantum yield: A comment on common ambiguity in the use of these optical concepts. *Limnol. Oceanogr.* **47**: 1261–1267.
- Jankowski, J. J., D. J. Kieber, and K. Mopper. 1999. Nitrate and nitrite ultraviolet actinometers. *Photochem. Photobiol.* **70**: 319–328. doi:[10.1111/j.1751-1097.1999.tb08143.x](https://doi.org/10.1111/j.1751-1097.1999.tb08143.x)
- Jankowski, J. J., D. J. Kieber, K. Mopper, and P. J. Neale. 2000. Development and intercalibration of ultraviolet solar actinometers. *Photochem. Photobiol.* **71**: 431–440. doi:[10.1562/0031-8655\(2000\)071<0431:DAIOUS>2.0.CO;2](https://doi.org/10.1562/0031-8655(2000)071<0431:DAIOUS>2.0.CO;2)
- Johannessen, S. C., and W. L. Miller. 2001. Quantum yield for the photochemical production of dissolved inorganic carbon in seawater. *Mar. Chem.* **76**: 271–283. doi:[10.1016/S0304-4203\(01\)00067-6](https://doi.org/10.1016/S0304-4203(01)00067-6)
- Kieber, D. J., G. W. Miller, P. J. Neale, and K. Mopper. 2014. Wavelength and temperature-dependent apparent quantum yields for photochemical formation of hydrogen peroxide in seawater. *Environ. Sci. Process. Impacts* **16**: 777–791. doi:[10.1039/c4em00036f](https://doi.org/10.1039/c4em00036f)
- Kirk, J. T. O. 1994. Light and photosynthesis in aquatic ecosystems, 2nd Edition. Cambridge Univ. Press.
- Koehler, B., E. Broman, and L. J. Tranvik. 2016. Apparent quantum yield of photochemical dissolved organic carbon mineralization in lakes. *Limnol. Oceanogr.* **61**: 2207–2221. doi:[10.1002/lno.10366](https://doi.org/10.1002/lno.10366)
- Koehler, B., T. Landelius, G. A. Weyhenmeyer, N. Machida, and L. J. Tranvik. 2014. Sunlight-induced carbon dioxide emissions from inland waters. *Global Biogeochem. Cycl.* **28**: 696–711. doi:[10.1002/2014GB004850](https://doi.org/10.1002/2014GB004850)
- Mannino, A., Novak, M. G., Nelson, N. B., Belz, M., Berthon J.-F., Blough N. V., Boss, E., Bricaud, A., Chaves, J., Del Castillo, C., Del Vecchio, R., D'Sa, E.J., Freeman, S., Matsuoka, A., Miller, R. L., Neeley, A., Röttgers, R., Tzortziou, M., and Werdell, J. 2019. Measurement protocol of absorption by chromophoric dissolved organic matter (CDOM) and other dissolved materials, In: *Inherent Optical Property Measurements and Protocols: Absorption Coefficient*, Mannino, A. and Novak, M. G. (eds.), IOCCG Ocean Optics and Biogeochemistry Protocols for Satellite Ocean Colour Sensor Validation, Volume 1.0, IOCCG, Dartmouth, NS, Canada.
- Miller, W. L., and R. G. Zepp. 1995. Photochemical production of dissolved inorganic carbon from terrestrial organic matter: Significance to the oceanic organic carbon cycle. *Geophys. Res. Lett.* **22**: 417–420. doi:[10.1029/94GL03344](https://doi.org/10.1029/94GL03344)
- Moran, M. A., W. M. Sheldon Jr., and R. G. Zepp. 2000. Carbon loss and optical property changes during long-term photochemical and biological degradation of estuarine dissolved organic matter. *Limnol. Oceanogr.* **45**: 1254–1264. doi:[10.4319/lo.2000.45.6.1254](https://doi.org/10.4319/lo.2000.45.6.1254)
- Murphy, K. R., K. D. Butler, R. G. M. Spencer, C. A. Stedmon, J. R. Boehme, and G. R. Aiken. 2010. Measurement of dissolved organic matter fluorescence in aquatic environments: An interlaboratory comparison. *Environ. Sci. Technol.* **44**: 9405–9412. doi:[10.1021/es102362t](https://doi.org/10.1021/es102362t)
- Ossola, R., O. M. Jönsson, K. Moor, and K. McNeill. 2021. Single oxygen quantum yields in environmental waters. *Chem. Rev.* **121**: 4100–4146. doi:[10.1021/acs.chemrev.0c00781](https://doi.org/10.1021/acs.chemrev.0c00781)
- Peacock, M., C. Freeman, V. Gauci, I. Lebron, and C. D. Evans. 2015. Investigations of freezing and cold storage for the analysis of peatland dissolved organic carbon (DOC) and absorbance properties. *Environ. Sci. Process. Impacts* **17**: 1290–1301. doi:[10.1039/c5em00126a](https://doi.org/10.1039/c5em00126a)
- Porcal, P., P. J. Dillon, and L. A. Molot. 2015. Temperature dependence of photodegradation of dissolved organic matter to dissolved inorganic carbon and particulate organic carbon. *PLoS One* **10**: e0128884. doi:[10.1371/journal.pone.0128884](https://doi.org/10.1371/journal.pone.0128884)
- Powers, L. C., J. A. Brandes, W. L. Miller, and A. Stubbins. 2017b. Using liquid chromatography-isotope ratio mass spectrometry to measure the $\delta^{13}\text{C}$ of dissolved inorganic carbon photochemically produced from dissolved organic carbon. *Limnol. Oceanogr. Methods* **15**: 103–115.
- Powers, L. C., J. A. Brandes, A. Stubbins, and W. L. Miller. 2017a. MoDIE: Moderate dissolved inorganic carbon (DI^{13}C) isotope enrichment for improved evaluation of DIC photochemical production in natural waters. *Mar. Chem.* **194**: 1–9.

- Powers, L. C., and W. L. Miller. 2015a. Photochemical production of CO and CO₂ in the Northern Gulf of Mexico: Estimates and challenges for quantifying the impact of photochemistry on carbon cycles. *Mar. Chem.* **171**: 21–35.
- Powers, L. C., and W. L. Miller. 2015b. Hydrogen peroxide and superoxide photoproduction in diverse marine waters: A simple proxy for estimating direct CO₂ photochemical fluxes. *Geophys. Res. Lett.* **42**: 7696–7704.
- R Development Core Team. 2014. R: A language and environment for statistical computing. R Foundation for Statistical Computing. doi:[10.4045/tidsskr.14.1316](https://doi.org/10.4045/tidsskr.14.1316)
- Ravichandran, M. 2004. Interactions between mercury and dissolved organic matter—A review. *Chemosphere* **55**: 319–331. doi:[10.1016/j.chemosphere.2003.11.011](https://doi.org/10.1016/j.chemosphere.2003.11.011)
- Raymond, P. A., and others. 2013. Global carbon dioxide emissions from inland waters. *Nature* **503**: 355–359. doi:[10.1038/nature12760](https://doi.org/10.1038/nature12760)
- Ren, C., G. Yang, and X. Lu. 2014. Autumn photoproduction of carbon monoxide in Jiaozhou Bay, China. *J. Ocean Univ. Chin.* **13**: 428–436. doi:[10.1007/s11802-014-2225-1](https://doi.org/10.1007/s11802-014-2225-1)
- Rundel, R. D. 1983. Action spectra and estimation of biologically effective UV radiation. *Physiol. Plant.* **58**: 360–366. doi:[10.1111/j.1399-3054.1983.tb04195.x](https://doi.org/10.1111/j.1399-3054.1983.tb04195.x)
- Sharp, J. H., R. Benner, L. Bennett, C. A. Carlson, S. E. Fitzwater, E. T. Peltzer, and L. M. Tupas. 1995. Analyses of dissolved organic carbon in seawater: the JGOFS EqPac methods comparison. *Mar. Chem.* **48**: 91–108. doi:[10.1016/0304-4203\(94\)00040-K](https://doi.org/10.1016/0304-4203(94)00040-K)
- Stauffer, R. E. 1990. Electrode pH error, seasonal epilimnetic pCO₂, and the recent acidification of the Maine lakes. *Water Air Soil Pollut.* **50**: 123–148.
- Timko, S. A., M. Gonsior, and W. J. Cooper. 2015. Influence of pH on fluorescent dissolved organic matter photo-degradation. *Water Res.* **85**: 266–274. doi:[10.1016/j.watres.2015.08.047](https://doi.org/10.1016/j.watres.2015.08.047)
- Vachon, D., J. F. Lapierre, and P. A. Giorgio. 2016. Seasonality of photochemical dissolved organic carbon mineralization and its relative contribution to pelagic CO₂ production in northern lakes. *Eur. J. Vasc. Endovasc. Surg.* **121**: 864–878. doi:[10.1002/2015JG003244](https://doi.org/10.1002/2015JG003244)
- Vähätalo, A. V., M. Salkinoja-Salonen, P. Taalas, and K. Salonen. 2000. Spectrum of the quantum yield for photochemical mineralization of dissolved organic carbon in a humic lake. *Limnol. Oceanogr.* **45**: 664–676. doi:[10.4319/lo.2000.45.3.0664](https://doi.org/10.4319/lo.2000.45.3.0664)
- Vähätalo, A. V., and R. G. Wetzel. 2004. Photochemical and microbial decomposition of chromophoric dissolved organic matter during long (months-years) exposures. *Mar. Chem.* **89**: 313–326. doi:[10.1016/j.marchem.2004.03.010](https://doi.org/10.1016/j.marchem.2004.03.010)
- Wang, W., C. G. Johnson, K. Takeda, and O. C. Zafiriou. 2009. Measuring the photochemical production of carbon dioxide from marine dissolved organic matter by pool isotope exchange. *Environ. Sci. Technol.* **43**: 8604–8609. doi:[10.1021/es901543e](https://doi.org/10.1021/es901543e)
- Ward, C. P., J. C. Bowen, D. H. Freeman, and C. M. Sharpless. 2021. Rapid and reproducible characterization of the wavelength dependence of aquatic photochemical reactions using light-emitting diodes. *Environ. Sci. Technol. Lett.* **8**: 437–442. doi:[10.1021/acs.estlett.1c00172](https://doi.org/10.1021/acs.estlett.1c00172)
- Ward, C. P., and R. M. Corry. 2020. Assessing the prevalence, products, and pathways of dissolved organic matter partial oxidation. *Environ. Sci. Process. Impacts* **22**: 1214–1223. doi:[10.1039/c9em00504h](https://doi.org/10.1039/c9em00504h)
- Ward, C. P., S. G. Nalven, B. C. Crump, G. W. Kling, and R. M. Cory. 2017. Photochemical alteration of organic carbon draining permafrost soils shifts microbial metabolic pathways and stimulates respiration. *Nat. Commun.* **8**: 1–8.
- White, E. M., D. J. Kieber, and K. Mopper. 2008. Determination of photochemically produced carbon dioxide in seawater. *Limnol. Oceanogr. Methods* **6**: 441–453. doi:[10.4319/lom.2008.6.441](https://doi.org/10.4319/lom.2008.6.441)
- Xiao, Y. H., T. Sara-Aho, H. Hartikainen, and A. V. Vähätalo. 2013. Contribution of ferric iron to light absorption by chromophoric dissolved organic matter. *Limnol. Oceanogr.* **58**: 653–662. doi:[10.4319/lo.2013.58.2.0653](https://doi.org/10.4319/lo.2013.58.2.0653)
- Xie, H., S. Bélanger, G. Song, R. Benner, A. Taalba, M. Blais, J. É. Tremblay, and M. Babin. 2012. Photoproduction of ammonium in the southeastern Beaufort Sea and its biogeochemical implications. *Biogeosciences* **9**: 3047–3061. doi:[10.5194/bg-9-3047-2012](https://doi.org/10.5194/bg-9-3047-2012)
- Xie, H., O. C. Zafiriou, W. J. Cai, R. G. Zepp, and Y. Wang. 2004. Photooxidation and its effects on the carboxyl content of dissolved organic matter in two coastal rivers in the southeastern United States. *Environ. Sci. Technol.* **38**: 4113–4119. doi:[10.1021/es035407t](https://doi.org/10.1021/es035407t)
- Zhang, Y., H. Xie, and G. Chen. 2006. Factors affecting the efficiency of carbon monoxide photoproduction in the St. Lawrence estuarine system (Canada). *Environ. Sci. Technol.* **40**: 7771–7777. doi:[10.1021/es0615268](https://doi.org/10.1021/es0615268)
- Zhu, X., W. L. Miller, and C. D. G. Fichot. 2020. Simple method to determine the apparent quantum yield matrix of CDOM photobleaching in natural waters. *Environ. Sci. Technol.* **54**: 14096–14106. doi:[10.1021/acs.est.0c03605](https://doi.org/10.1021/acs.est.0c03605)

Acknowledgments

We acknowledge funding by the Swedish Research Council for Environment, Agricultural Sciences and Spatial Planning (FORMAS) as part of the research environment “The Color of Water” (grant no. 2009-1350-15339-81) and by the Knut and Alice Wallenberg Foundation (Wallenberg Scholar KAW 2018-0191) to L.J.T.; by the Swedish Research Council (grant no. 2011-3475-604 88773-67) to L.J.T. and B.K.; by the Foundation King Carl XVI Gustaf 50-year Fond for Science, Technology and Environment 2015, and by the Matariki Network 2016 to B.K.; by the Science Council of the University of Jyväskylä for a mobility grant to Y.G.; by NSF grants OCE-0850677 to W.M. and OCE-1635618 to W.M. and L.P.; and by NSF CAREER 1351745 and the Camille and Henry

Dreyfus Foundation Postdoctoral Program in Environmental Chemistry to R.M.C. and C.P.W. Some materials in this manuscript are based on work supported while W.M. was serving at the U.S. National Science Foundation. We further acknowledge David J. Kieber for advice concerning nitrite actinometry.

Submitted 19 October 2021

Revised 04 March 2022

Accepted 11 March 2022

Associate editor: Hayley Schiebel